COx-free hydrogen production from ammonia – mimicking the activity of Ru catalysts with unsupported Co-Re alloys

Kirste, Karsten; McAulay, Kate; Bell, Tamsin E.; Stoian, Dragos; Laassiri, Said; Daisley, Angela; Hargreaves , Justin S.J.; Mathisen, Karina; Torrente-Murciano, Laura

COx-free hydrogen production from ammonia – mimicking the activity of Ru catalysts with unsupported Co-Re alloys

Karsten G. Kirste[a], Kate McAulay[b], Tamsin E. Bell[c], Dragos Stoian[d], Said Laassiri[b,e], Angela Daisley[b], Justin S.J. Hargreaves[b,*], Karina Mathisen[a,*], Laura Torrente-Murciano[c,*]

[a] Department of Chemistry, Norwegian University of Science and Technology, Høgskoleringen 5, N-7491, Trondheim, Norway
[b] Joseph Black Building, School of Chemistry, University of Glasgow, Glasgow, G12 8QQ, UK
[c] Department of Chemical Engineering and Biotechnology, University of Cambridge, Philippa Fawcett Drive, Cambridge, CB3 0AS, UK
[d] Swiss-Norwegian Beamlines, European Synchrotron Radiation Facility, F-38043, Grenoble cedex, France
[e] Chemical & Biochemical Sciences. Green Process Engineering (CBS). Mohamed VI Polytechnic University, UM6P, 43150, Ben Guerir, Morocco

ARTICLE INFO

ABSTRACT

On-demand production of hydrogen from ammonia is a challenge limiting the implementation of ammonia as a long term hydrogen vector to overcome the difficulties associated with hydrogen storage. Herein, we present the development of catalysts for the on-demand production of hydrogen from ammonia by combining metals with high and low N-adatom adsorption energies. In this way, cobalt-rhenium (Co-Re) catalysts show high activity mimicking that of ruthenium. EXAFS/XANES analyses demonstrate that the bimetallic Co-Re contribution is responsible for the activity and the stability of the catalysts in consecutive runs with no observable formation of nitrides (Co-N and Re-N) occurring under the ammonia atmosphere. While cobalt is partially re-oxidised under ammonia, re-reduction in the presence of rhenium is observed at higher temperatures, coinciding with the on-set of catalytic activity which is accompanied by minor structural changes. These results provide insight for the development of highly active alloy based ammonia decomposition catalysts.

1. Introduction

Ammonia is regarded as a safe and sustainable energy carrier due to its high hydrogen content and narrow flammable range [1,2] enabling the long term (days to months) energy storage in chemical bonds versus the short-term storage (seconds to hours) offered by electrochemical storage (i.e. batteries). In this way, the use of ammonia as an energy vector could facilitate the balance of seasonal energy demands and intermittent renewable energy production (e.g. solar, tidal and wind) in a carbon-free society [3–5]. Established safety protocols and existing transportation and distribution networks applicable for ammonia [6] make it also an effective possible solution in comparison to hydrogen due to the current lack of viable methods to store hydrogen in a compact, safe and cost-effective manner [7]. Despite its potential, the implementation of ammonia in the energy landscape relies on the capability of releasing hydrogen on-demand, preferably at temperatures aligned to those of fuel cells [8]. A considerable scientific effort is currently focused on the design of catalysts for the low temperature activation of ammonia for the production of hydrogen [2,9,10]. The most active catalysts reported in the literature are ruthenium-based

[11–16]. The optimum properties of ruthenium actives sites are associated with optimum N-adsorption energy [17] which enables activation of the ammonia molecule while avoiding poisoning by N-adatoms at low temperature (known to be the limiting step at such conditions). Enhancement of the ruthenium activity can be achieved by the use of electron donating promoters [11,13,18] and highly conductive supports, such as graphitised carbon nanotubes [19]. However, there is much interest in the identification of alternative catalysts which rival, if not exceed, the performance of ruthenium. Our recent review on the subject identifies cobalt as an attractive alternative, however studies show it to possess poor activity compared to ruthenium-based systems, especially at low temperatures [2,20–23]. The work reported within this manuscript demonstrates a systematic approach to replicate or improve upon the ammonia decomposition activity of ruthenium-based catalysts. The strategy employed by us has been the development of bimetallic systems combining metals possessing different N-adatom adsorption energies following the DFT simulations by Hangsen et al.[17] to achieve an optimum binding energy for catalytic performance. Within our studies, cobalt-rhenium systems present activity at conditions comparable to Ru/CNT catalysts [11] with very high stability

* Corresponding authors.
E-mail addresses: justinh@chem.gla.ac.uk (J.S.J. Hargreaves), karina.mathisen@ntnu.no (K. Mathisen), lt416@cam.ac.uk (L. Torrente-Murciano).

under consecutive runs and no observed formation of nitrides (Co-N and Re-N) under the ammonia atmosphere. Even though we recognise the scarcity and cost of Re, the knowledge provided in this study is useful for the development of catalysts of enhanced activity. The low temperature activity is directly related to the intimate Co-Re interaction with the activity onset related to the contraction of the Re-Co bond distance.

2. Experimental

2.1. Synthesis of catalysts

Cobalt rhenium materials were prepared to yield different Co/Re ratios, by mixing varying amounts of ammonium perrhenate (NH_4ReO_4, Sigma Aldrich, > 99%) in deionized water with cobalt nitrate (Co$(NO_3)_2$.6H$_2$O, Sigma Aldrich, > 98%). The solutions were stirred for 1 hour then dried in an oven at 125 °C for 12 hours. After drying, the materials were ground by hand and calcined in air at 700 °C (using a 10 °C min⁻¹ ramp rate) for 3 hours. Ruthenium supported on carbon nanotube (Ru/CNT) catalysts were prepared by incipient wetness impregnation using Ru(NO)(NO$_3$)$_3$ (Alfa Aesar). Multi-walled carbon nanotubes (Sigma Aldrich, OD 6-9 nm, length 5 μm, S$_{BET}$ 253 m^2 g^{-1}) were used as support. After impregnation of the aqueous solutions, the catalysts were dried at 100 °C under vacuum for 3 hours and then reduced under hydrogen at 230 °C for 1.5 hours.

Following degassing the materials, nitrogen physisorption isotherms were measured at −196 °C using a Micromeritics ASAP 2020 instrument. The surface area was calculated using the Brunauer, Emmett and Teller (BET) method. Temperature programmed reduction (TPR) experiments were carried out in a Micromeritics Autochem 2920 instrument equipped with a thermal conductivity detector (TCD). The samples characterised from room temperature to 900 °C using a temperature ramp rate of 10 °C min⁻¹ under 50 mL min⁻¹ flow of 5 % H$_2$/Ar. CO pulse chemisorption analyses at 35 °C were carried out using the Micromeritics Autochem 2920 instrument equipped with a TCD. Samples were pre-treated at 250 °C under a helium flow for 1 hour to ensure desorption of water.

2.2. XAS data collection

Cobalt K-edge and rhenium L$_{III}$-edge XAS data were collected at the Swiss-Norwegian Beamline (SNBL, BM1B) at the European Synchrotron Radiation Facility (ESRF) in transmission mode. The data was collected in the 16-bunch filling mode, providing a maximum current of 90 mA. A bending magnet collected the white beam from the storage ring to the beamline. The SNBL is equipped with a Si(111) double crystal monochromator for EXAFS data collection. The incident and transmitted intensities (I$_0$ and I$_t$ + I$_2$) were detected with ion chambers filled with, I$_0$ (17 cm) 50 % N$_2$ + 50 % He, and I$_t$ and I$_2$ (30 cm) with 85 % N$_2$ + 15 % Ar at the cobalt edge. Cobalt references (Co-foil, CoO, Co$_3$O$_4$) and rhenium references (Re-foil, NH$_4$ReO$_4$) were also collected. The cobalt K-edge XAS data were measured in continuous step scan mode from 7600 eV to 8300 eV with a step size of 0.5 eV and counting time of 300 ms per step. The rhenium L-III data were collected in transmission mode, using ion chambers fillings of 100 % N$_2$ (I$_0$, 17 cm), 50 % N$_2$ + 50 % Ar (I$_t$, 30 cm). Step scans were collected between 10350 eV to 11800 eV, with a step size of 0.5 eV and counting time of 200 ms per step.

For all *in situ* measurements, great care was taken to ensure similar conditions were applied for both edges, hence sample weight, cell thickness and gas flow were kept constant. The CoRe catalysts were mixed with boron nitride, pressed to wafers and sieved fractions (above 375 μm) were then placed inside 0.9 mm quartz capillaries with quartz wool on either side. The capillary was heated by a blower placed directly under the sample, and the exhaust was continuously sampled using a Pfeiffer Omnistar Mass Spectrometer. The protocol for the

ammonia decomposition includes pre-treatment in 75% H$_2$ in argon at 600 °C for one hour using a 5 °C min⁻¹ ramp rate using a total flow of 10 mL min⁻¹. EXAFS step scans were collected continuously, with XRD patterns being collected at end points. After the pre-treatment, samples were cooled to 200 °C before switching to 5% NH$_3$ in helium and heating to 700 °C using a ramp rate of 2 °C min⁻¹. EXAFS step scans were collected continuously, and the exhaust was continuously analysed using the mass spectrometer.

2.3. XAS data refinement

The XAS data were binned (edge region −30 eV to 50 eV; pre-edge grid 10 eV; XANES grid 0.5 eV; EXAFS grid 0.05 Å⁻¹) and background subtracted, and the EXAFS part of the spectrum extracted to yield the $\chi_i^{exp}(k)$ using Athena software from the IFFEFITT package. [24] The XANES spectra were normalised from 30 to 150 eV above the edge, while the EXAFS spectra were normalised from 150 eV to the end point. The data were carefully deglitched and truncated when needed. For cobalt the threshold energy (E$_0$) was set to be at the mid-point (0.5) of the normalised absorption edge step ensuring it was chosen after any pre-edge or shoulder features. For rhenium samples E$_0$ was determined to be the first inflection point in the first derivative spectra, as there are no pre-edges or shoulder features. All XANES spectra were energy corrected against the corresponding reference foil (Co = 7709 eV, Re = 10535 eV).

Due to the bimetallic nature of the CoRe-catalyst, as reported previously [25], obtaining accurate comparable results from linear combination of XANES using known references was difficult. For this reason, reduction and reaction profiles were obtained using multivariate curve resolution (MCR). MCR using the alternating least-square (ALS) mathematical algorithm is a chemometric method which is well-known for its ability to provide the pure response profile of the chemical constituent (species) of an unresolved mixture. Nowadays, MCR is heavily used as a blind source separation method (no reference spectra) to process large data-sets generated in labs and synchrotron facilities all over the world. For a detailed description of the method employed, software and usage, the reader is directed to literature from Jaumot et al. [26,27] and Ruckebush et al. [28] MCR-ALS was used to analyse the operando time-resolved (TR) XANES data-sets for Co-Re bimetallic catalysts during the pre-reduction step. For the assessment of the minimum number of principal components that describe the system, i.e. rank analysis, a built-in method based on the singular value decomposition (SVD) was used [29]. The SVD results display the calculated eigenvalues of the data versus the component number (a so-called scree plot), which allows understanding how much variance each component can explain. A break in the slope of such a plot is generally associated to the minimum number of components able to simulate the initial mixture. The MCR-ALS graphical user interface (GUI) for Matlab® used in the present manuscript (http://www.mcrals.info/) was applied on the XANES data-sets for both Co and Re edges (Co: 7600-8000 eV and Re: 10450-10800 eV). Positive constraints were utilised for both concentration and spectra profiles and closure constraints for the concentration (i.e. no mass transfer; constant concentration of the absorber throughout the experiment).

The peak fitting feature in the Athena software was used to calculate the area for the white line intensity at the Co K-edge for CoRe$_{1.6}$ during NH$_3$-treatment. A Gaussian curve was used to calculate the area. Difference spectra were made with the Athena software.

EXAFS least-squares refinements were carried out using DL-EXCURV [30], which conducts the curve fitting of the theoretical $\chi^{calc}(k)$ to the experimental $\chi^{exp}(k)$ using the curved wave theory. The fit parameter reported for each refinement procedure is given by the statistical R-factor, defined as:

$$R = \sum_i [(\chi_i^{exp} - \chi_i^{calc})k^{WT}]^2 / \sum_i [(\chi_i^{exp})k^{WT}]^2 x100\%$$

k^{WT} is the weight factor and a k^3-weighting was used for the analysed data. *Ab initio* phase shifts were also calculated within DL-EXCURV and verified using reference compounds. The least-squares refinements were carried out in typical wave number k range 2-8.5 Å^{-1} for cobalt and k range 3.5-9.5 Å^{-1} for rhenium using a k^3 weighting scheme.

Bimetallic fractions were calculated from the multiplicities of the Re L_{III}-edge from the EXAFS analysis after the method of Shibata et al. [31] The coordination number of the bimetallic contribution (N_{Re-Co}) was used to determine the ratio of bimetallic phase compared to the total coordination number (N_{Re-Re} + N_{Re-Co}).

2.4. Ammonia decomposition reaction

Ammonia decomposition reactions were carried out in a continuous differential packed bed reactor using 25 mg of catalyst diluted in a silicon carbide bed. The reactor system was equipped with mass flow and temperature controllers. The reaction tubing was heated to 60 °C to avoid ammonia condensation and consequent corrosion. Prior to each catalytic reaction study, the catalysts were pre-reduced *in situ* under a H$_2$ flow at 600 °C for 1 hour (unless otherwise stated). After pre-reduction, the temperature was returned to ambient under the H$_2$ flow. Following this, the reaction temperature was ramped from room temperature to 600 °C using a Carbolite tube furnace equipped with a PID controller. A 2.6 °C min^{-1} ramp under 2.5 mL min^{-1} NH$_3$ and 6 mL min^{-1} He (GHSV of 6000 mL$_{NH3}$·g$_{cat}$$^{-1}$ h^{-1}) was applied. The reactor exit gas was analysed using an on-line gas chromatograph fitted with a Porapak column and employing a thermal conductivity detector. Mass balance calculations were carried out to account for the molar expansion occurring as a result of the reaction. Mass balance was achieved within a ± 10 % error.

3. Results and discussion

A number of unsupported bimetallic combinations including CoRe$_{1.6}$, Ni$_2$Mo$_3$N, Co$_3$Mo$_3$N were tested for hydrogen production from ammonia decomposition (Fig. 1a) with the aim of achieving similar activities than the state-of-the-art ruthenium-based catalysts by combining transition metal catalysts with respectively higher and lower N-adatom adsorption energy than ruthenium. In addition to metal based catalysts, nitrides have also been investigated for ammonia decomposition, for example. [32,33] While Co-Mo alloy has been previously predicted as an optimum bimetallic combination [17,34,35], a considerably higher activity and, most importantly, an onset of activity at lower temperatures was achieved by the Co-Re alloy. Indeed, CoRe$_{1.6}$ has an activity comparable to 7 wt.% Ru/CNT [11]. 7 wt.% Ru/CNT is considered to be one of the optimum catalysts for this reaction due to the high concentration of B$_5$ sites (an arrangement of three Ru atoms in one layer and two further Ru atoms in the layer directly above) expressed in the 3.5-5 nm Ru nanoparticles present which are promoted by the CNT support [36]. While 3-5 nm supported Ru nanoparticles (7 wt.% Ru/CNT) present a considerably higher activity than the unsupported CoRe$_{1.6}$ per mol of metal (Fig. 1b), a rate a few orders of magnitude higher is shown by the CoRe$_{1.6}$ when activity is normalised by metallic surface area. It is important to highlight that the surface area of the unsupported CoRe$_{1.6}$ catalyst is only 0.2 m^2 g^{-1} as determined from the BET measurement (although the limitations in this regard with such a low surface area must be recognised) while the metallic surface area of the 7% Ru/CNT catalyst is 10 m^2 g^{-1} as measured by CO chemisorption. Pre-reduction in a H$_2$ flow was undertaken prior to surface area determination in both cases. Whilst the limitations of the BET method applied to CoRe$_{1.6}$ in view of its very low surface area are acknowledged, triplicate analyses confirmed the absence of micro- and meso-porosity. Considering the surface catalysed nature of ammonia decomposition, these results imply that the active sites in the Co-Re system might be considerably more active than those in their ruthenium counterparts. Both catalysts show a similar activation energy
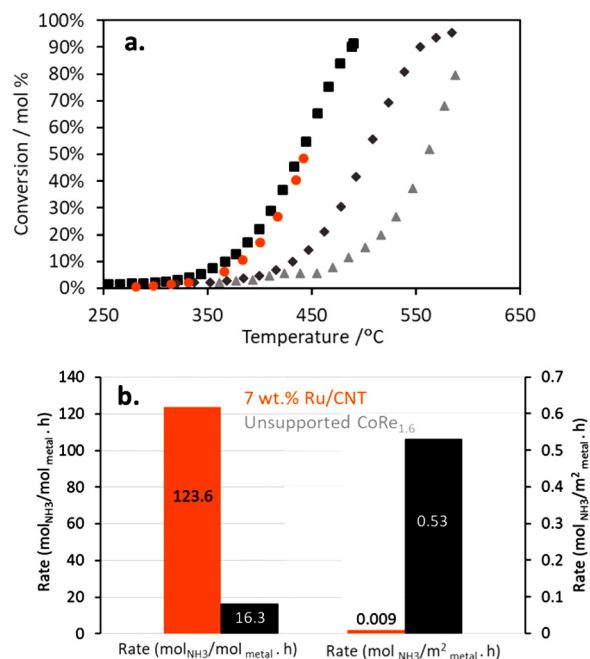

Fig. 1. (a) Catalytic activity of different alloy materials for the decomposition of ammonia. ■ CoRe$_{1.6}$ ▲ Ni$_2$Mo$_3$N ♦ Co$_3$Mo$_3$N ● 7% Ru/ CNT. Reaction conditions: 2.5 mL min^{-1} NH$_3$, 6 mL min^{-1} He, 25 mg catalyst, GHSV: 6000 h^{-1}. Catalysts are pre-reduced at 600 °C under H$_2$ flow. (b) Comparison of rate of reaction of 7 wt.% Ru/CNT (orange) and unsupported CoRe$_{1.6}$ (black) catalysts per mol of metal and per metallic surface area at 435 °C.

with values of 91 kJ mol^{-1} and 85 kJ mol^{-1} for 7 wt.% Ru/CNT and unsupported CoRe$_{1.6}$ respectively (the Arrhenius plots are available in the SI, Figure S1). These values are in agreement with those previously reported for Ru-based catalysts [11,19] and may possibly suggest similarities in the nature of the active sites in both systems, thereby confirming the potential of the design principle adopted, although this is a matter for further exploration.

As shown in Fig. 2, cobalt only and rhenium only counterpart catalysts show limited activity for ammonia decomposition demonstrating that the high activity of the CoRe$_{1.6}$ material is due to the synergetic effect achieved by the alloy formation [25].

The activity of the CoRe$_{1.6}$ catalyst was significantly increased as the pre-reduction temperature of the catalyst was increased (Fig. 3) from 400 to 600 °C. As the catalysts have been calcined at 700 °C under air, the role of pre-reduction is most likely not related to the promotion
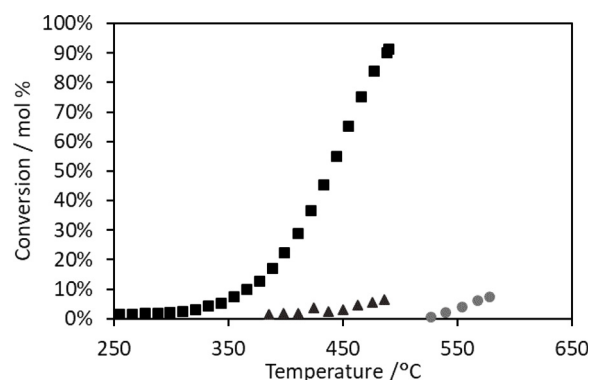

Fig. 2. Comparison of the catalytic activity of the CoRe$_{1.6}$ catalyst in comparison to materials prepared from the cobalt and rhenium precursors. ■ CoRe$_{1.6}$ ▲ Co(NO$_3$)$_2$·6H$_2$O derived material ● NH$_4$ReO$_4$ derived material. Reaction conditions: 2.5 mL min^{-1} NH$_3$, 6 mL min^{-1} He, 25 mg catalyst, GHSV: 6000 h^{-1}. Materials were pre-reduced at 600 °C under flowing H$_2$.
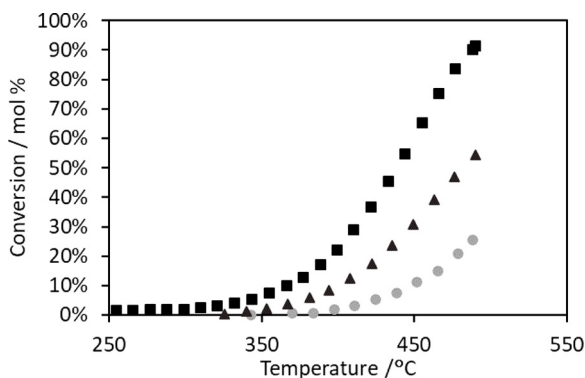
Fig. 3. Comparison of the catalytic activity of CoRe$_{1.6}$ catalyst pre-reduced under H$_2$ flow at ■ 600 °C ▲ 500 °C and ● 400 °C. Reaction conditions: 2.5 mL min^{-1} NH$_3$, 6 mL min^{-1} He, 25 mg catalyst, GHSV: 6000 h^{-1}.

of the thermal interaction between the Co and the Re atoms but rather the oxidation state of the active species. However, temperature programmed reduction (TPR) of the CoRe$_{1.6}$ catalyst (Figure S2 in the SI) reveals full reduction of both Co and Re components at 400 °C under hydrogen indicating that the apparent increase in catalytic activity at higher pre-reduction temperatures is likely to be associated with thermally-induced modifications in the bi-metallic material as evidenced below. For comparison, Figure S2 also shows the TPR of the calcined cobalt and rhenium precursors where full reduction requires temperatures of ~ 450-500 °C.

To gain a better understanding of the promotion of the interaction between the Co and Re during the pre-reduction of the CoRe$_{1.6}$ material, *in situ* X-ray absorption spectroscopy was applied. It is particularly applicable to the current study where there could be concerns that the *ex situ* nature of the material may differ from that under reaction conditions. Attention was particularly directed to the near edge (XANES) region as it is highly sensitive to the local environment and oxidation state. Fig. 4 reveals that a cobalt intermediate state is formed during reduction at temperatures above 100 °C comprising an apparent mixture of Co^{2+} and Co^0 species. Full reduction to Co^0 occurs over a narrow temperature window starting at 350 °C with the final reduced state being complete at 400 °C. Reduction of rhenium occurs abruptly and in one step initiating at 300 °C. Fig. 5 presents spectra determined

at different stages of the activation and reaction process.

During heating of the CoRe$_{1.6}$ catalyst in 5% NH$_3$, partial oxidation of cobalt is evident by the increased white line intensity observed between 200-400 °C [37,38](Fig. 5c), as in agreement with supported CoRe in a silica aerogel. [39] Even if changes were observed in the more sensitive XANES for cobalt, EXAFS analysis (Table 1) revealed no light atom scattering pairs (i.e. Co-N) formed during the low-temperature ammonia treatment. Hence, any oxidation must be limited to the surface which would be difficult to distinguish in the EXAFS analysis of CoRe$_{1.6}$. Starting at 400 °C during ammonia treatment, the white line intensity (Fig. 5d) gradually decreased reaching a similar intensity at 600 °C as observed for CoRe$_{1.6}$ during pre-treatment. This corresponds to a partial reduction of cobalt coinciding with CoRe$_{1.6}$ becoming active for ammonia decomposition. Interestingly, no changes were observed in the XANES region (Figure S3 in the SI) for rhenium during ammonia decomposition. These observations are in agreement with the widespread use of Re as a promoter in cobalt-based catalysts for the Fischer-Tropsch reaction where it facilitates not only Co reduction but also retards its sintering [40].

Results from EXAFS analysis (Table 1) and average coordination numbers for the unsupported CoRe$_{1.6}$ catalysts from pre-reduction between 400-600 °C show an average multiplicity of the Co-Co pair between 3.5 and 4 at around 2.45 Å, while the first Re-Re shell at 2.64 -2.69 Å contains on average 6-7 neighbours. While no Co-Re contribution could be fitted, a small Re-Co contribution could refined between 2.55-2.57 Å with an average multiplicity between 1.2-1.4. Attempts were made to refine the corresponding Co-Re shell, however they were not successful. This can be explained by Co-Co and Co-Re backscattering pairs having similar bond distances which were not resolved by our limited Δk-window. Attempts were also made to include mixed site option in the EXCURV software, essentially forcing Co-Co and Co-Re shells to have the same bond length, however, this did not improve the fit-factor and therefore the Co-Re contribution was removed. It is believed that the refinement of the Co-Re contribution is limited by the experimental constraints, i.e. filling mode (16-bunch), high rhenium content and elevated temperatures. EXAFS refinements indicated a complete reduction of CoRe$_{1.6}$ from 400 °C in 75% H$_2$ as no metal-O pairs could be fitted, in agreement with the TPR results described above. The addition of a metal-O pair in the fitting model for Fig. 6a) and Fig. 7a) produced no valid results and did not improve the fit. This reveals that the major contributing species formed during pre-treatment
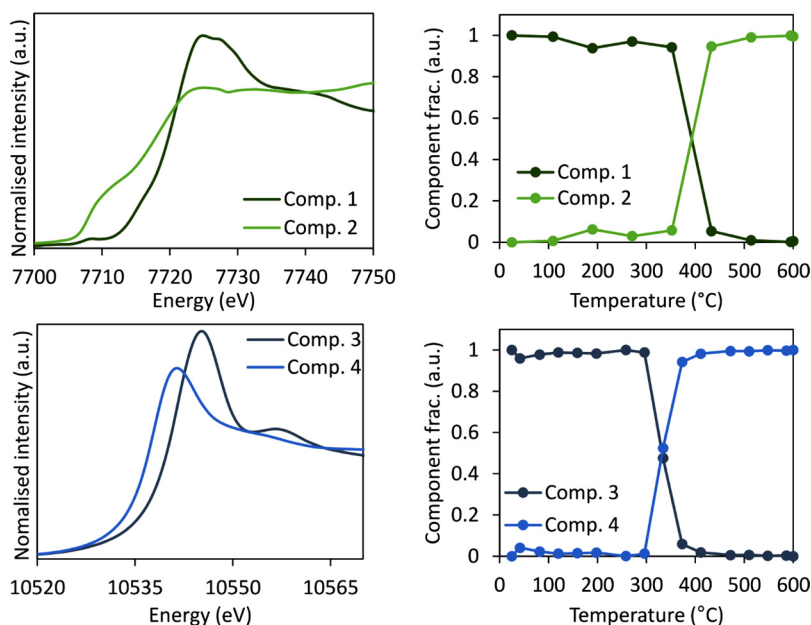

Fig. 4. Reduction of CoRe$_{1.6}$ at Co K-edge (top) and Re L$_{III}$-edge (bottom) described with MCR analysis of the unsupported CoRe$_{1.6}$ catalyst.
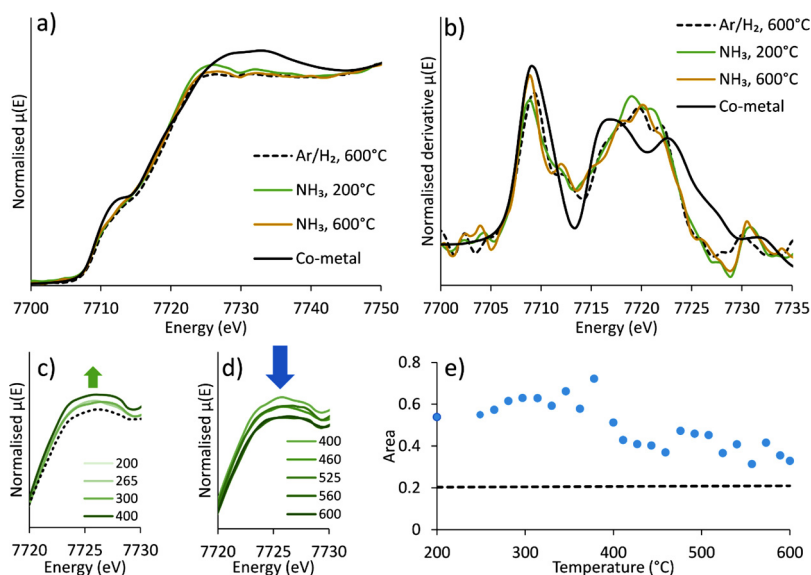
Fig. 5. a) XANES of CoRe$_{1.6}$ from the Co K-edge comparing the end of the pre-treatment, the beginning and the end of the NH$_3$-treatment with metallic cobalt. b) The first derivative of the XANES of CoRe$_{1.6}$ from the Co K-edge. c) White line intensity changes due to partial oxidation during NH$_3$-treatment from 200-400 °C of CoRe$_{1.6}$ (The reduced in 75% H$_2$/Ar CoRe$_{1.6}$ (…) is added for comparison) d) Re-reduction of Co in CoRe$_{1.6}$ shown by decreasing white line intensity from the Co K-edge from 400-600 °C. e) Area for the white line intensity for cobalt in CoRe$_{1.6}$ at the Co-edge plotted versus temperature.

Table 1

EXAFS least squares refinements of CoRe$_{1.6}$ after Ar/H$_2$ PT and ammonia decomposition at the Co L$_{III}$-edge and Re L$_{III}$-edge from *in situ* XAS[a]. AFAC taken from Co-foil = 0.79 and Re-foil = 0.80.

Treatment	Shell	N	R/Å	$2\sigma^2$/Å^2	E_F/eV	R/%	$\Delta\kappa$
Ar/H$_2$, 400 °C	Co-Co	4(1)	2.45(1)	0.020(7)	9(1)	49	2-8
	Re-Co	1.3(7)	2.57(1)	0.01(1)	−7(5)	58	3.5-9.5
	Re-Re	7(5)	2.64(9)	0.05(2)			
Ar/H$_2$, 500 °C	Co-Co	3.5(9)	2.44(1)	0.019(6)	9.35	42	2-8
	Re-Co	1.2(4)	2.55(1)	0.012(5)	−10(1)	33	3.5-9.5
	Re-Re	7(3)	2.68(2)	0.05(1)			
Ar/H$_2$, 600 °C	Co-Co	4(1)	2.45(2)	0.026(7)	−2(2)	45	2-8
	Re-Co	1.4(7)	2.55(1)	0.022(8)	−10(3)	42	3.5-9.5
	Re-Re	6(3)	2.69(6)	0.04(1)			
NH$_3$, 300 °C	Co-Co	4(1)	2.45(2)	0.023(8)	3(2)	43	2-8
	Re-Co	1.6(7)	2.61(1)	0.030(9)	−9(2)	31	3.5-9.5
	Re-Re	3.3(9)	2.65(1)	0.018(5)			
NH$_3$, 400 °C	Co-Co	4(1)	2.45(2)	0.024(7)	3(2)	39	2-8
	Re-Co	1.3(5)	2.56(1)	0.018(7)	−9(2)	35	3.5-9.5
	Re-Re	6(2)	2.68(3)	0.034(8)			
NH$_3$, 500 °C	Co-Co	4(1)	2.44(2)	0.025(7)	3(2)	38	2-8
	Re-Co	0.9(3)	2.563(8)	0.009(6)	−10(2)	32	3.5-9.5
	Re-Re	7(2)	2.70(4)	0.043(9)			
NH$_3$, 600 °C	Co-Co	3.4(9)	2.45(2)	0.021(6)	2(2)	39	2-8
	Re-Co	1.4(8)	2.57(1)	0.02(1)	−11(3)	51	3.5-9.5
	Re-Re	6(3)	2.73(5)	0.04(1)			

of CoRe$_{1.6}$ are Co-Co and Re-Re with only ~20% of the bimetallic Re-Co pair.

After cooling and switching to 5% NH$_3$, partial oxidation of Co was observed in the XANES, however this was not reflected in the EXAFS (at 300 °C) where four Co-Co pairs at 2.45 Å were found similarly to the pre-treatment. A better fit was obtained at the Re L$_{III}$-edge at lower temperatures yielding an average of 3.3 Re-Re backscattering pairs at 2.65 Å. We believe the lowered multiplicity originates from better accuracy and is not a reflection of reduction in particle size. The Re-Co bimetallic pair remained but at an elongated bond distance of 2.61 Å with a slightly increased average multiplicity to 1.6. Hence, there were minor structural changes observed in the EXAFS for CoRe$_{1.6}$ when switching from a hydrogen to an ammonia atmosphere (Fig. 6 and Fig. 7)

When increasing the temperature from 300 °C to 600 °C under the ammonia atmosphere, the Co-Co backscattering pair was surprisingly stable (Fig. 8 and Fig. 9) despite the observed partial oxidation and re-reduction observed in the XANES. These observations align with the excellent stability of the CoRe$_{1.6}$ catalysts under consecutive reaction

runs as shown below. The average Co-Co multiplicity remained at 4 with a bond distance of 2.45 Å throughout the ammonia treatment. This contrasts with the Re-Re backscattering shell where significant elongation of bond distance from 2.65 Å to 2.73 Å was observed (Fig. 9) during ammonia decomposition. Great care must be taken when comparing coordination shell distances from EXAFS at different temperatures, as other effects, such as thermal expansion, may contribute to the observed changes. [41] While multiplicities of Re-Re, Re-Co and Co-Co remained constant after the reduction stage, we observed variations in bond distances for these coordination shells as mentioned above. Fig. 9 illustrates these changes, ΔR, for these shells during pre-treatment and ammonia decomposition. During the pre-treatment step, relative changes of the first metal coordination shells were apparent relative to their initial appearance (400 °C), while relative changes during ammonia decomposition were shown in relation to the pre-treated sample. While the Co-Co bond distance remained unchanged during pre-treatment, an observed elongation of the Re-Re bond (2.65-2.69 Å) concurs with a slight contraction of the Re-Co bond (2.57-2.55 Å). This strongly indicates that local restructuring of both monometallic and bimetallic particles occurs between 400-600 °C, after TPR and MCR data suggest CoRe$_{1.6}$ is fully reduced. After switching to ammonia at 200 °C the Re-Re bond was significantly shortened to 2.65 Å and the Re-Co distance is elongated (2.61 Å). During ammonia decomposition however these two distances were separated as Re-Re increased to 2.73 Å, while Re-Co was shortened (2.56 Å) coinciding with CoRe$_{1.6}$ becoming active. While the observed elongation in bond distance approaches that of Re-foil (2.74 Å), it did not seem to be associated with sintering of a pure Re-Re phase in CoRe$_{1.6}$ as the average multiplicity remained between 6-7 similarly to that observed in the H$_2$ pre-treatment. Similar bond distances (2.56-2.57 Å) were found for rhenium promoted Co/Al$_2$O$_3$ during CO oxidation by *in situ* XAS. [42]

It should be noted that higher order cumulants [43] (C$_3$ and C$_4$) were introduced during EXAFS refinements, however they did not improve the fits for either rhenium or cobalt. Somewhat ordered higher coordination shells are observed at the Co K-edge (Fig. 6) at low temperatures during pre-treatment, but these could not be fitted. However, these shells seem to disintegrate at higher temperatures and during ammonia treatment. Higher coordination shells were not observed at the Re L$_{III}$-edge (Fig. 7) at any reaction stage. This indicates a high degree of disorder in the CoRe$_{1.6}$ during ammonia treatment. This is also the case for the material for ammonia synthesis. [25]

It is of interest to monitor the bimetallic Re-Co contribution during the reaction stages and we have included two methods where we utilise information from XANES and EXAFS. Bimetallic fractions calculated
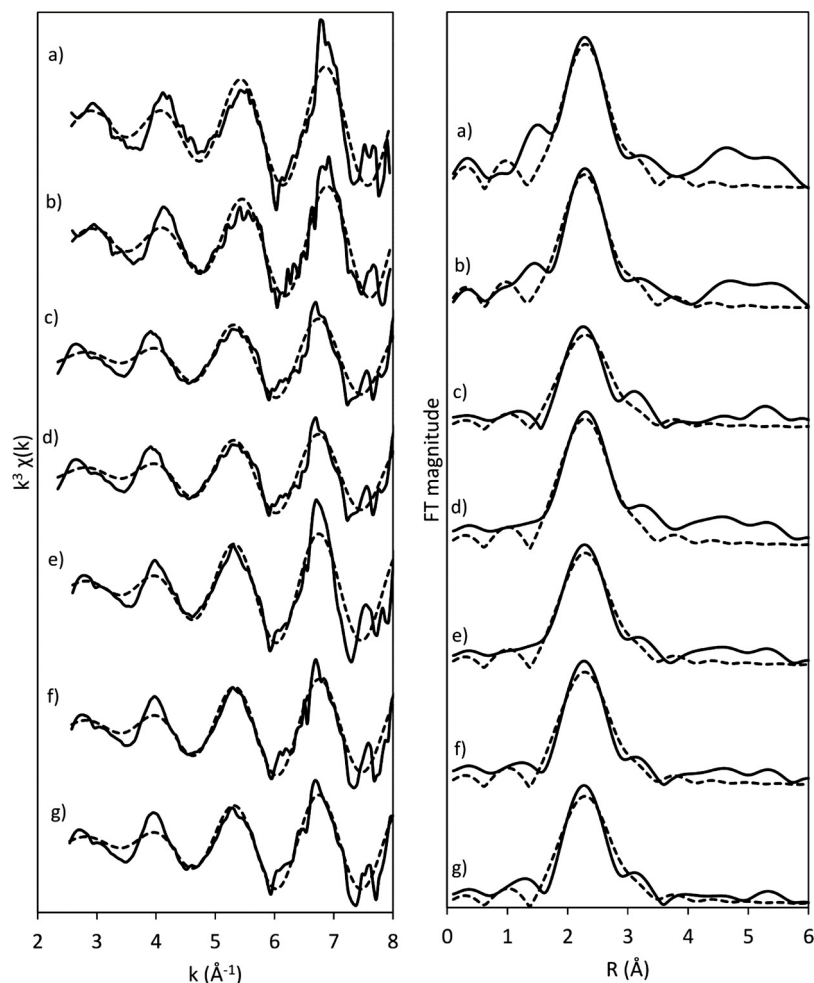
Fig. 6. Experimental (—) and calculated (—) k^3-weighted EXAFS (left) and its Fourier Transform (right) for $CoRe_{1.6}$ during pre-treatment in Ar/H_2 from 400-600 °C and NH_3 decomposition from 300-600 °C for the Co K-edge. a) 400 °C in H_2/Ar, b) 500 °C in H_2/Ar, c) 600 °C in H_2/Ar, d) 300 °C in NH_3, e) 400 °C in NH_3, f) 500 °C in NH_3, and g) 600 °C in NH_3.

from EXAFS (Fig. 10, bottom) are somewhat stable between 0.1 and 0.3 through the reaction stages. However, due to high uncertainties of the Re-Re multiplicities especially, the XANES has been examined to look for features associated with the Re-Co bimetallic pair. The difference spectra (Fig. 10, top, black line) between Co-foil and the pre-treated $CoRe_{1.6}$ show several features, one at 7712 eV associated with the pre-edge and a negative peak at 7722 eV together with a peak at 7730 eV related to the white line. Of these, the feature at 7712 eV would be more characteristic for assigning Re-Co bimetallic species, as the latter two can also be affected by oxidation and reduction processes. The feature at 7760 eV will be affected by temperature and particle size and is therefore less reliable for this purpose. The difference spectra for $CoRe_{1.6}$ during ammonia treatment (Fig. 10, top, green line) monitor possible changes in the XANES compared to the final state at 600 °C in ammonia. It is evident that there are no significant changes in bimetallic Re-Co contribution during the process, rather the observed changes are attributed to partial oxidation and re-reduction.

These results are similar to the behaviour of $CoRe_{1.6}$ during ammonia synthesis where the Ar/H_2 pre-treated material shows a stable bimetallic fraction throughout the process. [25] The complete reduction observed from the lack of Co-O and Re-O interactions in the EXAFS confirms that all of the metal is in the metallic state, and while the system is made up of Co-Co, Re-Re and Co-Re/Re-Co coordination pairs, the local structure of each particle is more difficult to predict.

Results from XAS reveals that the $CoRe_{1.6}$ catalyst remains largely unchanged during the ammonia treatment. This also precludes nitride formation as no Co-N/Re-N coordination shells were found during any stage of the process with the interaction with reactants and products

The stable Co-Re contributions are in agreement with the excellent stability of the unsupported $CoRe_{1.6}$ catalysts in at least 6 consecutive ammonia decomposition runs up to 500 °C where the temperature is returned to ambient values after each run before being increased again (Fig. 11).

4. Conclusions

This paper provides new information for the development of active ammonia decomposition catalysts using bi-metallic combinations. Unsupported CoRe catalysts present an ammonia decomposition activity comparable to the state-of-the-art Ru-based systems with high stability under consecutive runs. The high activity is related to the bimetallic Co-Re contribution with no significant change across the studied temperatures with the exception of partial oxidation and re-reduction of the cobalt species. The re-reduction in the presence of the Re component coincides with the onset of ammonia decomposition activity. In addition, no Co-N or Re-N backscattering shells are found during EXAFS analysis under ammonia atmosphere. In terms of the CoRe catalyst, future attention should be directed towards the application of supports to increase the dispersion of the active phase and also to the application of potential promoters, whilst recognising the relative high cost of the Re component.
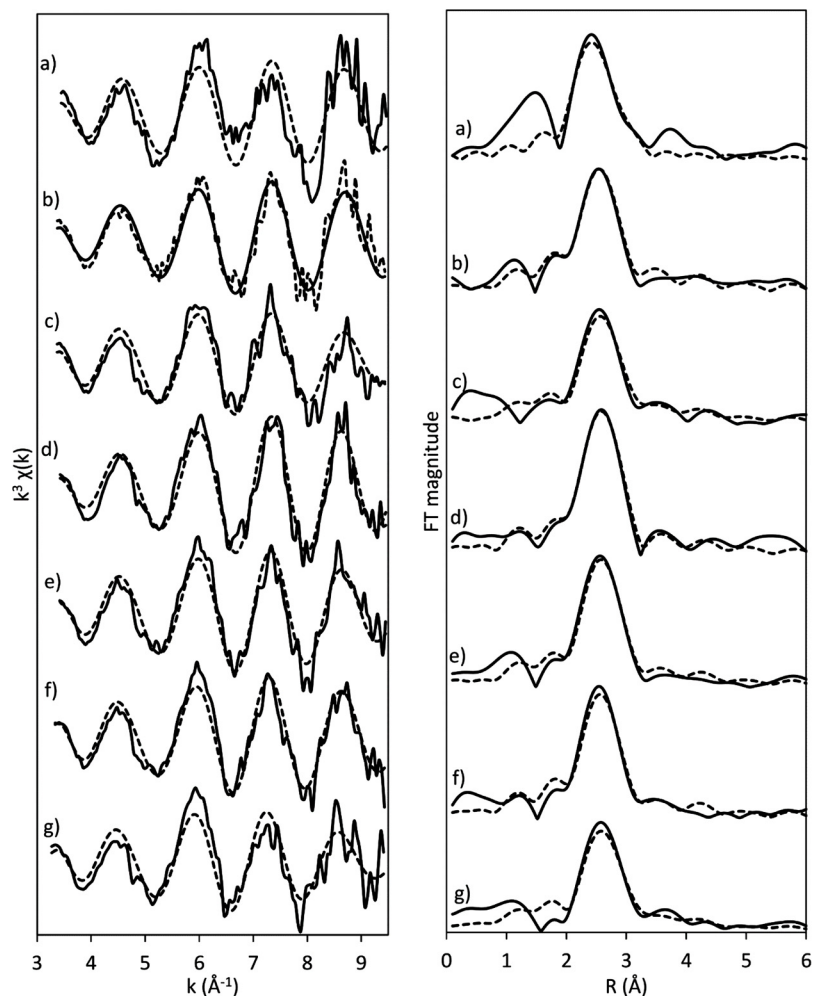
Fig. 7. Experimental (—) and calculated (—) k^3-weighted EXAFS (left) and its Fourier Transform (right) for $CoRe_{1.6}$ during pre-treatment in Ar/H_2 from 400-600 °C and NH_3 decomposition from 300-600 °C for the Re L_{III}-edge. a) 400 °C in H_2/Ar, b) 500 °C in H_2/Ar, c) 600 °C in H_2/Ar, d) 300 °C in NH_3, e) 400 °C in NH_3, f) 500 °C in NH_3, and g) 600 °C in NH_3.

CRediT authorship contribution statement

Karsten G. Kirste: Investigation, Data curation, Writing - original draft, Writing - review & editing. **Kate McAulay:** Investigation, Writing - review & editing. **Tamsin E. Bell:** Investigation, Data curation, Writing - original draft, Writing - review & editing. **Dragos Stoian:** Investigation. **Said Laassiri:** Investigation, Writing - review & editing. **Angela Daisley:** Investigation, Writing - review & editing. **Justin S.J. Hargreaves:** Supervision, Funding acquisition, Writing - review & editing. **Karina Mathisen:** Supervision, Funding acquisition, Writing -
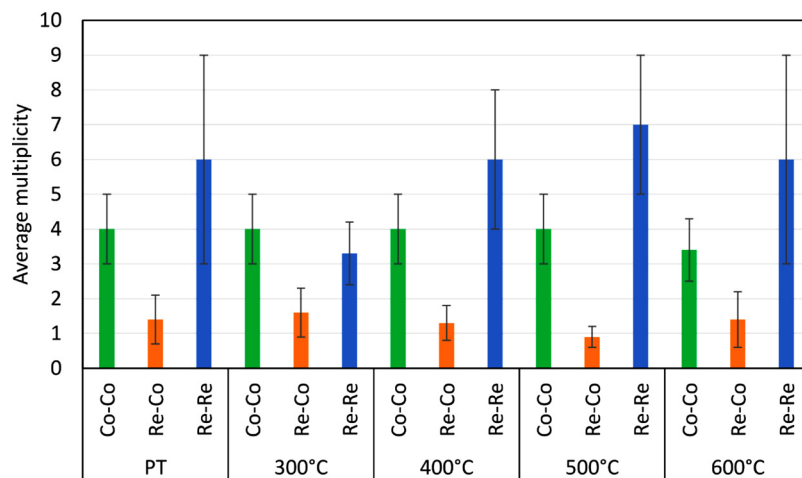
Fig. 8. Average coordination numbers (N) from EXAFS analysis for $CoRe_{1.6}$ after 60 min pre-treatment at 600 °C in H_2/Ar (left), and during heating in 5% NH_3 for Co K-edge and Re L_{III}-edge at selected temperatures.
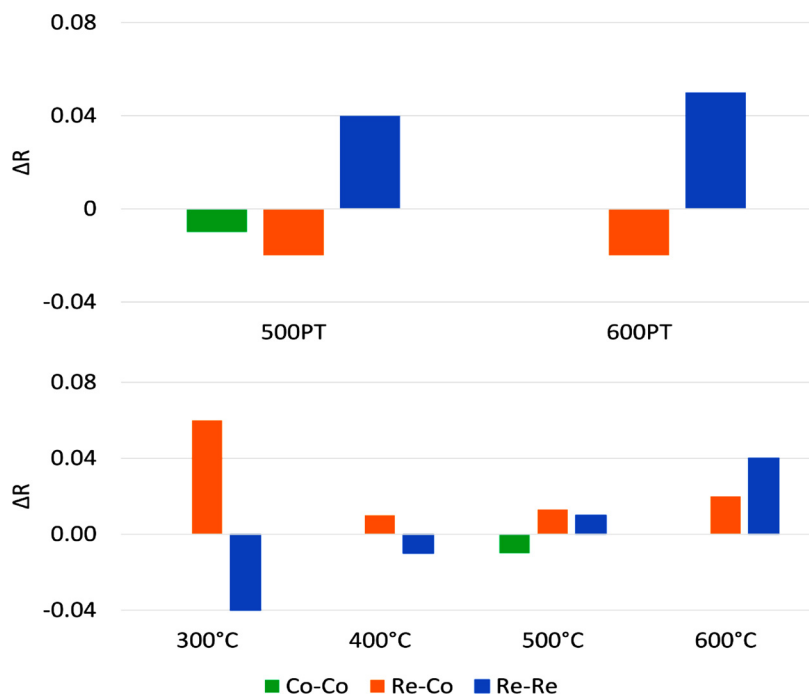
Fig. 9. Variations in bond distances (Å) determined from EXAFS refinements for CoRe$_{1.6}$ during pre-treatment compared to the pre-treatment stage at 400 °C in H$_2$/Ar (top) and ammonia decomposition compared to the pre-treatment stage at 600 °C in H$_2$/Ar (bottom).
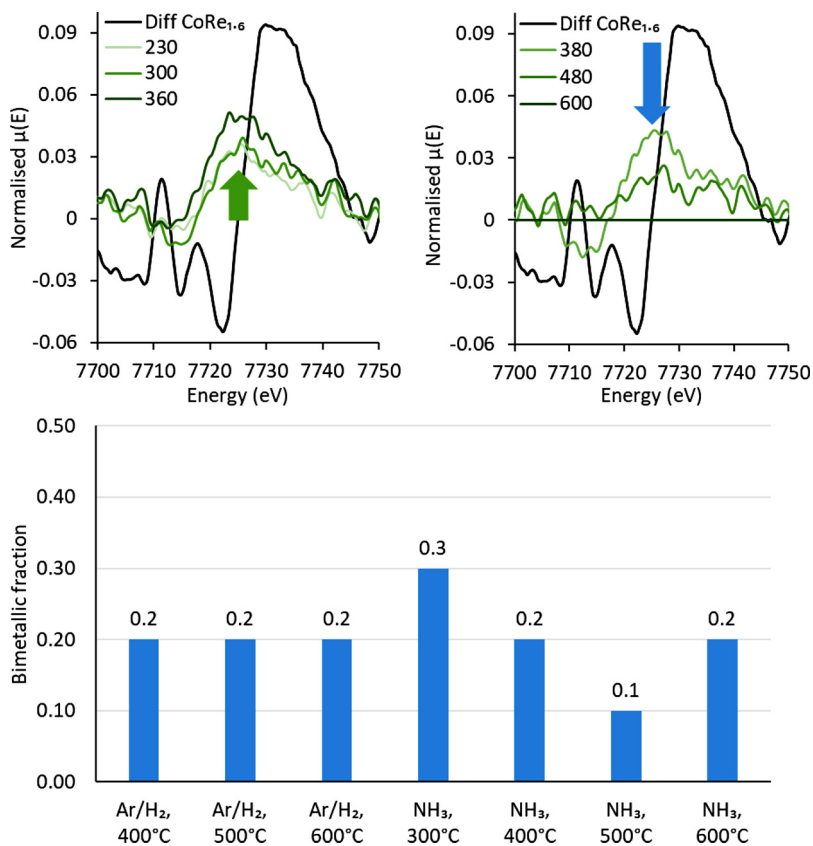

Fig. 10. Top: Difference spectrum between Co-foil and pre-treated CoRe$_{1.6}$ (black) compared to difference spectra of CoRe$_{1.6}$ during ammonia treatment compared with the final state at 600 °C in 5% NH$_3$ (green). Bottom: Calculated bimetallic fractions from EXAFS refinements from Re L$_{III}$-edge.
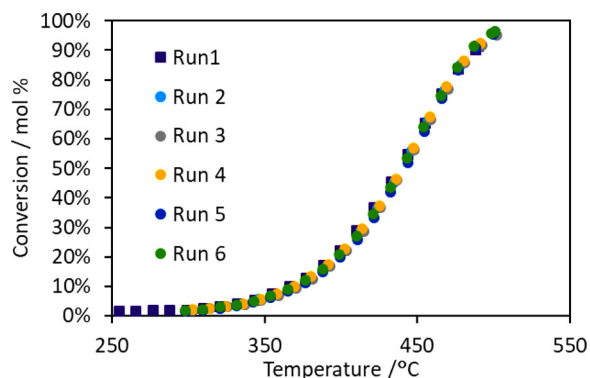
Fig. 11. Consecutive ammonia decomposition catalytic runs using unsupported CoRe$_{1.6}$ catalyst pre-reduced under H$_2$ flow at 600 °C. Reaction conditions: 2.5 mL min^{-1} NH$_3$, 6 mL min^{-1} He, 25 mg catalyst, GHSV: 6000 h^{-1}.

original draft, Writing - review & editing. **Laura Torrente-Murciano:** Supervision, Funding acquisition, Writing - original draft, Writing - review & editing.

Declaration of Competing Interest

The authors report no declarations of interest.

Acknowledgments

Appendix A. Supplementary data

Supplementary material related to this article can be found, in the online version, at doi:https://doi.org/10.1016/j.apcatb.2020.119405.

References

[1] R.F. Service, Liquid sunshine, Science 361 (6398) (2018) 120–123.
[2] T.E. Bell, L. Torrente-Murciano, H2 Production via Ammonia Decomposition Using Non-Noble Metal Catalysts: A Review, Top Catal 59 (15-16) (2016) 1438–1457.
[3] C. Zamfirescu, I. Dincer, Ammonia as a green fuel and hydrogen source for vehicular applications, Fuel Process. Technol. 90 (5) (2009) 729–737.
[4] A. Klerke, C.H. Christensen, J.K. Norskov, T. Vegge, Ammonia for hydrogen storage: challenges and opportunities, Journal of Materials Chemistry 18 (20) (2008) 2304–2310.
[5] C. Smith, A.K. Hill, L. Torrente-Murciano, Current and future role of Haber-Bosch ammonia in a carbon-free energy landscape, Energy Environ. Sci. (2020).
[6] G. Thomas, G. Parks, Potential roles of ammonia in a hydrogen economy, Technical report. U.S. Department of Energy (2006).
[7] M.P. Suh, H.J. Park, T.K. Prasad, D.W. Lim, Hydrogen storage in metal-organic frameworks, Chem Rev 112 (2) (2012) 782–835.
[8] U. D. o. Energy, Targets for Onboard Hydrogen Storage Systems for Light-Duty Vehicles, http://energy.gov/eere/fuelcells/downloads/targets-onboard-hydrogen-storage-systems-light-duty-vehicles.
[9] F. Schuth, R. Palkovits, R. Schlogl, D.S. Su, Ammonia as a possible element in an energy infrastructure: catalysts for ammonia decomposition, Energy Environ. Sci. 5 (4) (2012) 6278–6289.
[10] S.F. Yin, B.Q. Xu, X.P. Zhou, C.T. Au, A mini-review on ammonia decomposition catalysts for on-site generation of hydrogen for fuel cell applications, Appl. Catal. A-Gen. 277 (1-2) (2004) 1–9.
[11] A.K. Hill, L. Torrente-Murciano, In-situ H-2 production via low temperature decomposition of ammonia: Insights into the role of cesium as a promoter, International Journal of Hydrogen Energy 39 (15) (2014) 7646–7654.
[12] T.E. Bell, G.W. Zhan, K.J. Wu, H. Zeng, L. Torrente-Murciano, Modification of

[13] Ammonia Decomposition Activity of Ruthenium Nanoparticles by N-Doping of CNT Supports, Top Catal 60 (15-16) (2017) 1251–1259.
[13] D.C. Huang, C.H. Jiang, F.J. Liu, Y.C. Cheng, Y.C. Chen, K.L. Hsueh, Preparation of Ru-Cs catalyst and its application on hydrogen production by ammonia decomposition, International Journal of Hydrogen Energy 38 (8) (2013) 3233–3240.
[14] F.R. Garcia-Garcia, J. Alvarez-Rodriguez, I. Rodriguez-Ramos, A. Guerrero-Ruiz, The use of carbon nanotubes with and without nitrogen doping as support for ruthenium catalysts in the ammonia decomposition reaction, Carbon 48 (1) (2010) 267–276.
[15] W. Rarog-Pilecka, E. Miskiewicz, S. Jodzis, J. Petryk, D. Lomot, Z. Kaszkur, Z. Karpinski, Z. Kowalczyk, Carbon-supported ruthenium catalysts for NH3 synthesis doped with caesium nitrate: Activation process, working state of Cs-Ru/C, Journal of Catalysis 239 (2) (2006) 313–325.
[16] Z. Hu, J. Mahin, S. Datta, T.E. Bell, L. Torrente-Murciano, Ru-Based Catalysts for H2 Production from Ammonia: Effect of 1D Support, Top Catal (2018).
[17] D.A. Hansgen, D.G. Vlachos, J.G. Chen, Using first principles to predict bimetallic catalysts for the ammonia decomposition reaction, Nat Chem 2 (6) (2010) 484–489.
[18] Z. Hu, J. Mahin, L. Torrente-Murciano, A MOF-templated approach for designing ruthenium–cesium catalysts for hydrogen generation from ammonia, International Journal of Hydrogen Energy 44 (57) (2019) 30108–30118.
[19] A.K. Hill, L. Torrente-Murciano, Low temperature H2 production from ammonia using ruthenium-based catalysts: Synergetic effect of promoter and support, Applied Catalysis B: Environmental 172-173 (2015) 129–135 (0).
[20] L. Torrente-Murciano, A.K. Hill, T.E. Bell, Ammonia decomposition over cobalt/carbon catalysts-Effect of carbon support and electron donating promoter on activity, Catalysis Today 286 (2017) 131–140.
[21] H. Zhang, Y.A. Alhamed, A. Al-Zahrani, M. Daous, H. Inokawa, Y. Kojima, L.A. Petrov, Tuning catalytic performances of cobalt catalysts for clean hydrogen generation via variation of the type of carbon support and catalyst post-treatment temperature, International Journal of Hydrogen Energy 39 (31) (2014) 17573–17582.
[22] Z. Lendzion-Bielun, R. Pelka, W. Arabczyk, Study of the Kinetics of Ammonia Synthesis and Decomposition on Iron and Cobalt Catalysts, Catalysis Letters 129 (1-2) (2009) 119–123.
[23] H.A. Lara-Garcia, J.A. Mendoza-Nieto, H. Pfeiffer, L. Torrente-Murciano, COx-free hydrogen production from ammonia on novel cobalt catalysts supported on 1D titanate nanotubes, International Journal of Hydrogen Energy 44 (57) (2019) 30062–30074.
[24] B. Ravel, M. Newville, ATHENA, ARTEMIS, HEPHAESTUS: data analysis for X-ray absorption spectroscopy using IFEFFIT, J Synchrotron Radiat 12 (Pt 4) (2005) 537–541.
[25] K. Mathisen, K.G. Kirste, J.S.J. Hargreaves, S. Laassiri, K. McAulay, A.R. McFarlane, N.A. Spencer, An In Situ XAS Study of the Cobalt Rhenium Catalyst for Ammonia Synthesis, Top Catal 61 (3) (2018) 225–239.
[26] J. Jaumot, R. Gargallo, A. de Juan, R. Tauler, A graphical user-friendly interface for MCR-ALS: a new tool for multivariate curve resolution in MATLAB, Chemometrics and Intelligent Laboratory Systems 76 (1) (2005) 101–110.
[27] J. Jaumot, A. de Juan, R. Tauler, MCR-ALS GUI 2.0: New features and applications, Chemometrics and Intelligent Laboratory Systems 140 (2015) 1–12.
[28] C. Ruckebusch, L. Blanchet, Multivariate curve resolution: a review of advanced and tailored applications and challenges, Anal Chim Acta 765 (2013) 28–36.
[29] A. Martini, E. Borfecchia, K.A. Lomachenko, I.A. Pankin, C. Negri, G. Berlier, P. Beato, H. Falsig, S. Bordiga, C. Lamberti, Composition-driven Cu-speciation and reducibility in Cu-CHA zeolite catalysts: a multivariate XAS/FTIR approach to complexity, Chemical Science 8 (10) (2017) 6836–6851.
[30] S. Tomic, B.G. Searle, A. Wander, N.M. Harrison, A.J. Dent, J.F.W. Mosselmans, J.E. Inglesfield, New Tools for the Analysis of EXAFS: The DL EXCURV Package. CCLRC Technical Report 2005, Council for the Central Laboratory of the Research Councils, UK, 2020.
[31] T. Shibata, B.A. Bunker, Z. Zhang, D. Meisel, C.F. Vardeman 2nd, J.D. Gezelter, Size-dependent spontaneous alloying of Au-Ag nanoparticles, J Am Chem Soc 124 (40) (2002) 11989–11996.
[32] S.F. Zaman, L.A. Jolaoso, S. Podila, A.A. Al-Zahrani, Y.A. Alhamed, H. Driss, M.M. Daous, L. Petrov, Ammonia decomposition over citric acid chelated γ-Mo2N and Ni2Mo3N catalysts, International Journal of Hydrogen Energy 43 (36) (2018) 17252–17258.
[33] L.A. Jolaoso, S.F. Zaman, S. Podila, H. Driss, A.A. Al-Zahrani, M.A. Daous, L. Petrov, Ammonia decomposition over citric acid induced γ-Mo2N and Co3Mo3N catalysts, International Journal of Hydrogen Energy 43 (10) (2018) 4839–4844.
[34] C.J. Jacobsen, S. Dahl, B.S. Clausen, S. Bahn, A. Logadottir, J.K. Norskov, Catalyst design by interpolation in the periodic table: bimetallic ammonia synthesis catalysts, J Am Chem Soc 123 (34) (2001) 8404–8405.
[35] J. Ji, X.Z. Duan, G. Qian, X.G. Zhou, G.S. Tong, W.K. Yuan, Towards an efficient CoMo/gamma-Al2O3 catalyst using metal amine metallate as an active phase precursor: Enhanced hydrogen production by ammonia decomposition, International Journal of Hydrogen Energy 39 (24) (2014) 12490–12498.
[36] F.R. Garcia-Garcia, A. Guerrero-Ruiz, I. Rodriguez-Ramos, Role of B5-Type Sites in Ru Catalysts used for the NH3 Decomposition Reaction, Top Catal 52 (6-7) (2009) 758–764.
[37] F. Carraro, O. Vozniuk, L. Calvillo, L. Nodari, C. La Fontaine, F. Cavani, S. Agnoli, In operando XAS investigation of reduction and oxidation processes in cobalt and iron mixed spinels during the chemical loop reforming of ethanol, Journal of Materials Chemistry A 5 (39) (2017) 20808–20817.
[38] A. Moen, D.G. Nicholson, B.S. Clausen, P.L. Hansen, A. Molenbroek, G. Steffensen, X-ray Absorption Spectroscopic Studies at the Cobalt K-Edge on a Reduced Al2O3-Supported Rhenium-Promoted Cobalt Fischer−Tropsch Catalyst, Chemistry of

Materials 9 (5) (1997) 1241–1247.

[39] K.G. Kirste, S. Laassiri, Z. Hu, D. Stoian, L. Torrente-Murciano, J.S.J. Hargreaves, K. Mathisen, XAS investigation of silica aerogel supported cobalt rhenium catalysts for ammonia decomposition, Physical Chemistry Chemical Physics (2020), https://doi.org/10.1039/d0cp00558d.

[40] G. Jacobs, J.A. Chaney, P.M. Patterson, T.K. Das, B.H. Davis, Fischer–Tropsch synthesis: study of the promotion of Re on the reduction property of Co/Al2O3 catalysts by in situ EXAFS/XANES of Co K and Re LIII edges and XPS, Applied Catalysis A: General 264 (2) (2004) 203–212.

[41] L.-G. Liu, T. Takahashi, W.A. Bassett, Effect of pressure and temperature on the

lattice parameters of rhenium, Journal of Physics and Chemistry of Solids 31 (6) (1970) 1345–1351.

[42] A. Voronov, N.E. Tsakoumis, N. Hammer, W. van Beek, H. Emerich, M. Rønning, The state and location of Re in Co–Re/Al2O3 catalysts during Fischer–Tropsch synthesis: Exploring high-energy XAFS for in situ catalysts characterisation, Catalysis Today 229 (2014) 23–33.

[43] T. Kristiansen, J.A. Stovneng, M.A. Einarsrud, D.G. Nicholson, K. Mathisen, There and Back Again: The Unique Nature of Copper in Ambient Pressure Dried-Silica Aerogels, Journal of Physical Chemistry C 116 (38) (2012) 20368–20379.